

**SUBSEQUENT COMPARISON OF MEASUREMENTS OF NEUTRON SOURCE
EMISSION RATE (2016-17) – CCRI(III)-K9.AmBe.2**

N.J. Roberts*

National Physical Laboratory (NPL), Teddington, UK

C. Thiam

*Université Paris-Saclay, CEA, List, Laboratoire National Henri Becquerel (LNE-LNHB),
F-91120, Palaiseau, France*

M. Capogni and L. Silvi

*ENEA - Istituto Nazionale di Metrologia delle Radiazioni Ionizzanti (INMRI), Centro Ricerche
Casaccia, I-00123 Santa Maria di Galeria (Roma), Italy*

* corresponding author: neil.roberts@npl.co.uk

ABSTRACT

Section III (neutron measurements) of the Comité Consultatif des Rayonnements Ionisants, CCRI, conducted a subsequent comparison of primary measurements of the neutron emission rate of an $^{241}\text{Am-Be}(\alpha,n)$ radionuclide source. The aim of this comparison was to compare primary measurements of the neutron emission rate of an $^{241}\text{Am-Be}(\alpha,n)$ radionuclide source for laboratories who were outliers in the previous comparison (K9.AmBe) or who were unable to participate. Three laboratories participated – LNHB (France), ENEA-INMRI (Italy) and NPL (UK) – with NPL as the pilot institute and the link to the K9.AmBe comparison. Measurements were made in 2016-17. Each laboratory reported the neutron emission rate into 4π sr together with a detailed uncertainty budget. All participants used the manganese bath technique.

TABLE OF CONTENTS

1	Introduction.....	4
2	The $^{241}\text{Am-Be}(\alpha, n)$ radionuclide source	4
3	Neutron emission rate measurement techniques of the laboratories	4
3.1	ENEA	4
3.2	LNHB	5
3.3	NPL	5
4	Measurements	6
4.1	Emission rates as reported by participants	6
4.2	Degree of equivalence between participants	7
4.3	Using same oxygen (n, α) cross-section evaluation	8
5	Link with CCRI(III)-K9.AmBe	9
6	Summary and Conclusion	10
7	Acknowledgements	11
8	Appendices	12
8.1	Uncertainty Budgets	12
8.2	Anisotropy measurements	13
8.2.1	LNHB	13
8.2.2	NPL	13
8.2.3	Results	14
9	References	15

1 INTRODUCTION

It is the aim of CCRI Section III to compare the realisation of standards of all relevant neutron quantities over a ten year cycle. Each comparison exercise should take less than four years from initial planning to publication of report in open literature. The previous comparison of measurements of source emission rate started in 1999 and took six years to complete¹. The main reasons for this extended schedule were the difficulties in transporting radioactive sources between countries and also the request of some participants to receive the source for a second measurement.

The aim of this comparison is to compare primary measurements of the neutron emission rate of an $^{241}\text{Am-Be}(\alpha, n)$ radionuclide source for laboratories who were outliers in the previous comparison (K9.AmBe) or who were unable to participate. The NPL was the pilot institute and, as a participant in the previous key comparison K9.AmBe, provided a link to that exercise.

Three laboratories were scheduled to participate:

Ente per le Nuove Tecnologie, l'Energia e l'Ambiente - Istituto Nazionale di Metrologia delle Radiazioni Ionizzanti (ENEA-INMRI), Rome, Italy

Laboratoire National Henri Becquerel (LNE-LNHB), Paris-Saclay, France

National Physical Laboratory (NPL), Teddington, UK

2 THE $^{241}\text{Am-Be}(\alpha, n)$ RADIONUCLIDE SOURCE

The neutron source used was a sealed $^{241}\text{Am-Be}(\alpha, n)$ source (model Am1.N09, serial number 002/07) owned by LNHB, which had a nominal activity of 11 GBq. It is in a cylindrical capsule (outer length 19.2 mm, outer diameter 17.4 mm) and was manufactured by Eckert and Zielger Cesio.

The source was chosen as it is a similar type as that used in the K9.AmBe comparison. It has a long half-life and stable decay process, and also because it is representative of the type and size of neutron sources commonly used at the present time in calibration laboratories. After LNHB had made the first measurement the source was sent to NPL in 2017. The source was then sent from NPL to ENEA-INMRI later in 2017 and returned to LNHB in the same year.

In 2018 a provisional notification of results was provided to LNHB, at their request, which contained the degree of equivalence between LNHB and NPL, the associated expanded uncertainty and the normalised error.

3 NEUTRON EMISSION RATE MEASUREMENT TECHNIQUES OF THE LABORATORIES

3.1 ENEA-INMRI

The ENEA-INMRI manganese bath is a stainless steel sphere 100 cm in diameter and 5 mm thick, containing solution with a density of 1.280 g cm^{-3} and an impurity level of 0.00778 %.

The neutron source was placed in the centre of the bath in a spherical Plexiglass container with a radius of 4.87 cm. After 24 hours the source was removed and a NaI(Tl) scintillation detector was introduced at the approximate centre of the bath. Gamma spectra were recorded for 13 hours in 1 hour acquisitions and the count rate obtained by setting a window from 38.24 to 1854.64 keV.

The efficiency of the ENEA-INMRI manganese bath system was determined using a concentrated ^{56}Mn solution, standardized by the ENEA-INMRI secondary standard (well-type ionization chamber) previously calibrated by using several absolute techniques based on coincidence counting, CIEMAT/NIST and TDCR methods.

The probability of neutron capture by ^{55}Mn nuclei was evaluated directly using Fluka² simulations with ENDF/B-VI cross-sections. The separate components for neutron leakage, fast neutron losses due to interactions in the oxygen and sulphur, and thermal neutrons absorbed by the neutron source and the container were also evaluated although were not used in the calculation of the emission rate.

3.2 LNHB

The LNHB manganese bath is a thin-walled stainless steel sphere of 100 cm in diameter, filled with a solution of manganese sulphate with a density of 1.277 g cm^{-3} (measured with a calibrated densitometer). The experimental set up is described in references 3 and 4.

The neutron source was placed in the centre of the bath in a cylindrical PMMA holder. The solution was stirred and circulated continuously between the bath and a detector assembly containing a 4"×4" NaI(Tl) scintillation detector which is used to measure the induced activity of ^{56}Mn at saturation.

The detector assembly was last calibrated at LNHB in 2012 using a concentrated ^{56}Mn solution, standardized by the TDCR (triple to double coincidence ratio) method in order to determine the efficiency of the LNHB manganese bath system.

The probability of neutron capture by the manganese in the solution was calculated using MCNP6⁵ with ENDF/B-VII cross-sections. Corrections were made for neutron leakage, fast neutron losses due to interactions in the oxygen and sulphur, and thermal neutrons absorbed by the neutron source and the container.

3.3 NPL

The NPL manganese bath is a sphere of 98 cm in diameter. Solution with a hydrogen to manganese number density ratio ($N_{\text{H}}/N_{\text{Mn}}$) of 34.38 was used, the concentration of which was determined gravimetrically.

The solution was continuously circulated through a shielded reservoir where two $\phi 50\text{ mm} \times 50\text{ mm}$ NaI scintillators were used to measure the activity of the solution, before being pumped back into the bath. The saturated count rate was obtained from the counting cycles when the source was in the bath as well as from those after the source had been removed. Both NPL measurements consisted of two separate bath irradiations performed within a week of each other.

The NaI detectors were calibrated by adding an active solution of ^{56}Mn to the bath, the activity concentration of which had been determined by ionisation chamber counting at NPL. The active solution was produced by irradiating a bottle of MnSO_4 solution extracted from the bath in the NPL thermal pile.

MCNP5 was used to calculate the leakage fraction, the capture in the source and source mounting assembly, and the capture by (n,p) and (n, α) reactions in sulphur and oxygen using ENDF/B-VI cross-sections where available. Thermal neutron capture by hydrogen, sulphur, and solution

impurities was calculated using thermal cross sections with appropriate Westcott parameters to allow for epithermal resonance capture. A hydrogen to manganese cross-section ratio derived from measurements in the NPL manganese bath was used. The impurity levels were taken from a chemical analysis of the solution.

Table 1: Summary of manganese bath parameters

Laboratory	Bath size	N_H/N_{Mn} at time of measurement	Correction factor method	Oxygen cross-section	Impurities considered?	Activity counting system
ENEA-INMRI	100 cm diameter	51.5	FLUKA	ENDF/B-VI	Yes	Static, NaI in bath
LNHB	100 cm diameter	52.2	MCNP6	ENDF/B-VII	No	Circulation of solution
NPL	98 cm diameter	34.28	MCNP5+thermal calculation	ENDF/B-VI	Yes	Circulation of solution

Where not provided by the participants, values of N_H/N_{Mn} were calculated from the solution density using the model of Laliberté and Cooper⁶.

4 MEASUREMENTS

4.1 Emission rates as reported by participants

The emission rates submitted by each participant with uncertainties at $k = 2$ are given in Table 2. All values have been corrected to the reference date of 1st January 2016. After submitting their initial results, ENEA-INMRI were asked to check their analysis for errors, due to the disagreement between the ENEA-INMRI and NPL emission rates, but without being told the magnitude or direction of the difference. In response, ENEA-INMRI provided a revised emission rate. After the provisional notification of results had been provided, LNHB identified a discrepancy with the solution concentration in their MCNP model used to derive the correction factors which would increase the reported emission rate by 0.39 %. As this came after LNHB were aware of the results, the revised emission rate has not been considered in this report, but it is included in Table 2 for completeness.

Table 2: Emission rates corrected to 1st January 2016 with uncertainties at $k = 2$

Laboratory	Emission rate ($\times 10^5 \text{ s}^{-1}$)	Uncertainty [$k = 2$] ($\times 10^5 \text{ s}^{-1}$)
ENEA-INMRI	3.949	0.085
LNHB	3.364	0.076
LNHB (revised*)	3.377	0.076
NPL	3.448	0.048

* The LNHB revised value was not considered as their reported value.

The results are plotted in Figure 1 with uncertainties at the $k = 2$ level.

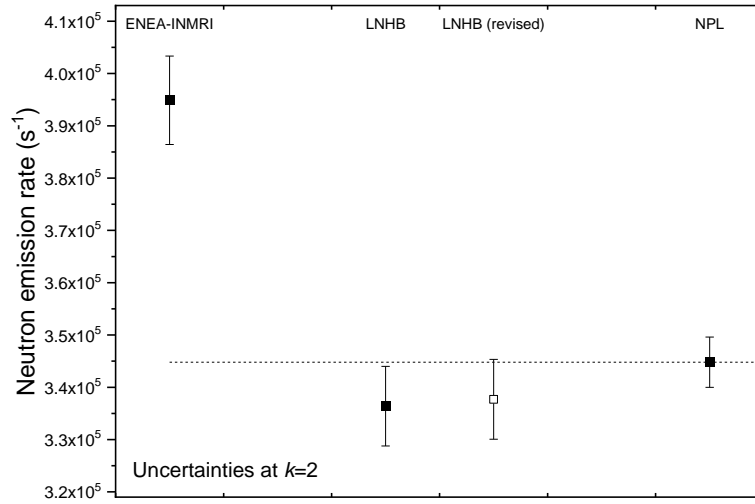


Figure 1: Graph of emission rates with uncertainties at $k=2$. The revised LNHB value is plotted for completeness.

4.2 Degree of equivalence between participants

Before linking the present measurements to the initial K9.AmBe comparison exercise, the results from each participant were compared with the NPL value to evaluate the level of agreement. The degree of equivalence (DoE) between NPL and the two participating laboratories was calculated as the difference between the values of emission rate (Q) reported by the participants

$$D_{NPL,participant} = Q_{NPL} - Q_{participant} \quad (1)$$

with the expanded uncertainty as follows

$$U(D_{NPL,participant}) = 2\sqrt{u^2(Q_{NPL}) + u^2(Q_{participant})} \quad (2)$$

For the above formula, the correlation between results reported by NPL and the participants are considered not significant. The normalised error (En) in the DoE was then calculated as follows

$$En = \frac{|D_{NPL,participant}|}{U(D_{NPL,participant})} \quad (3)$$

A value of En in the range 0 to 1 indicates that the difference between the measured values of the participating laboratories is less than or equal to the combined expanded uncertainties of the two laboratories.

The degrees of equivalence with the associated uncertainty is given in Table 3.

Table 3: Degrees of equivalence between NPL and ENEA, and NPL and LNHB

Participant	$D_{NPL,participant}$	$U(D_{NPL,participant})$	En
ENEA-INMRI	$-5.009 \times 10^4 \text{ s}^{-1}$	$9.719 \times 10^3 \text{ s}^{-1}$	5.154
LNHB	$8.400 \times 10^3 \text{ s}^{-1}$	$8.998 \times 10^3 \text{ s}^{-1}$	0.934

The results presented in Figure 1 and Table 3 indicate that the measurements by LNHB and NPL are in agreement, but that by ENEA-INMRI is not in agreement with the NPL value.

4.3 Using same oxygen (n, α) cross-section evaluation

It is well known that the choice of O(n, α) cross-section has a significant influence on the neutron emission rate obtained from the manganese bath technique, the influence being around 0.8 % between ENDF/B-VI.0 and ENDF/B-VII.0^{7,8}. LNHB used the ENDF/B-VII.0 evaluation, whereas NPL used the ENDF/B-VI.0 evaluation, so to quantify the influence of the O(n, α) cross-section on the level of agreement the NPL results were recalculated using correction factors based on ENDF/B-VII.0 evaluations. The NPL values obtained using both cross-section evaluations are plotted alongside the LNHB value in Figure 2. The ENEA results were derived using the same cross-sections as NPL so they were not considered in this section.

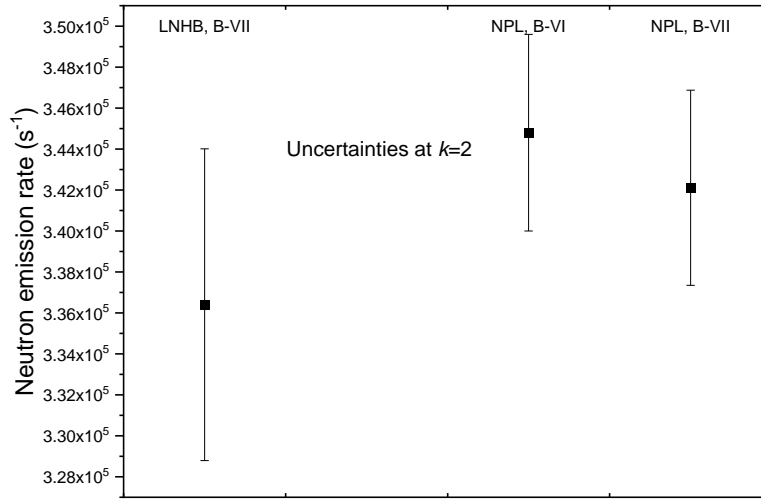


Figure 2: Graph of emission rates, including the NPL rate using correction factors based on ENDF/B-VII cross-sections, with uncertainties at $k = 2$

The degree of equivalence when both laboratories use the same oxygen cross-section data is given in Table 4.

Table 4: Degree of equivalence between NPL and LNHB when both use the same oxygen cross section data

$D_{NPL, LNHB}$	$U(D_{NPL, LNHB})$	En
$5.711 \times 10^3 \text{ s}^{-1}$	$8.979 \times 10^3 \text{ s}^{-1}$	0.636

The degree of equivalence and the normalised error have reduced showing that the two values are still in agreement when normalised to the same oxygen cross-section data. The reduction in the degree of equivalence of $2.689 \times 10^3 \text{ s}^{-1}$ has the same magnitude as the reduction in the NPL measured rate when the ENDF/B-VII evaluation is used, which corresponds to a 0.78 % reduction in the source emission rate. In keeping with the approach taken for the original CCRI(III).K9.AmBe evaluation, the degrees of equivalence for this exercise are based on the reported values of the participants regardless of which cross-sections were used in their analysis.

4.4 Long term stability of the NPL Mn bath

NPL routinely measures the emission rates of its neutron sources both to confirm the decay is as expected and to confirm the long-term stability of the manganese bath system. The decay-corrected emission rates of 5 Am-based sources are plotted in Figure 3 for the period from 1997 to 2017,

covering the K9.AmBe and K9.AmBe.2 exercises. Source number 1096 was the Am-Be source used in the K9.AmBe comparison.

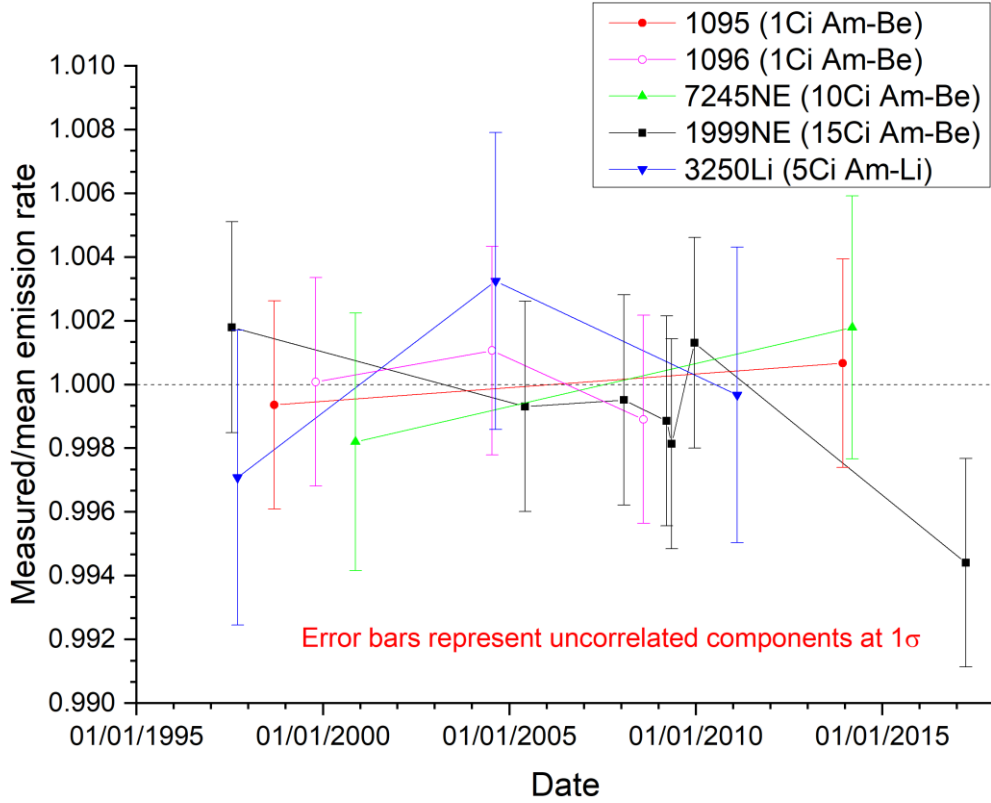


Figure 3: Normalised decay-corrected measurements of Am-based neutron source emission rates at NPL over the period between the K9.AmBe and K9.AmBe.2 comparison exercises

5 LINK WITH CCRI(III)-K9.AMBE

The new results obtained by LNHB and ENEA-INMRI can be linked to the CCRI(III)-K9.AmBe reference value via the NPL results. The ratio of the participant's value in this comparison to that of NPL in this comparison can be multiplied by the NPL value from the original CCRI(III)-K9.AmBe comparison to yield the linked value for the participant ($Q_{participant,K9.AmBe}$) as shown in equation 4.

$$Q_{participant,K9.AmBe} = Q_{NPL,K9.AmBe} \frac{Q_{participant,K9.AmBe.2}}{Q_{NPL,K9.AmBe.2}} \quad (4)$$

The linked values can then be used to derive the unilateral degrees of equivalence and associated uncertainties linked to the CCRI(III)-K9.AmBe KCRV. These are given in Table 5 and plotted alongside the DoEs for the other participants in the CCRI(III)-K9.AmBe exercise in Figure 4.

Table 5: Unilateral degrees of equivalence linked to the CCRI(III)-K9.AmBe KCRV

Participant	$D_{participant}$	$U(D_{participant})$
ENEA-INMRI	$0.3406 \times 10^6 \text{ s}^{-1}$	$0.0800 \times 10^6 \text{ s}^{-1}$
LNHB	$-0.0719 \times 10^6 \text{ s}^{-1}$	$0.0706 \times 10^6 \text{ s}^{-1}$

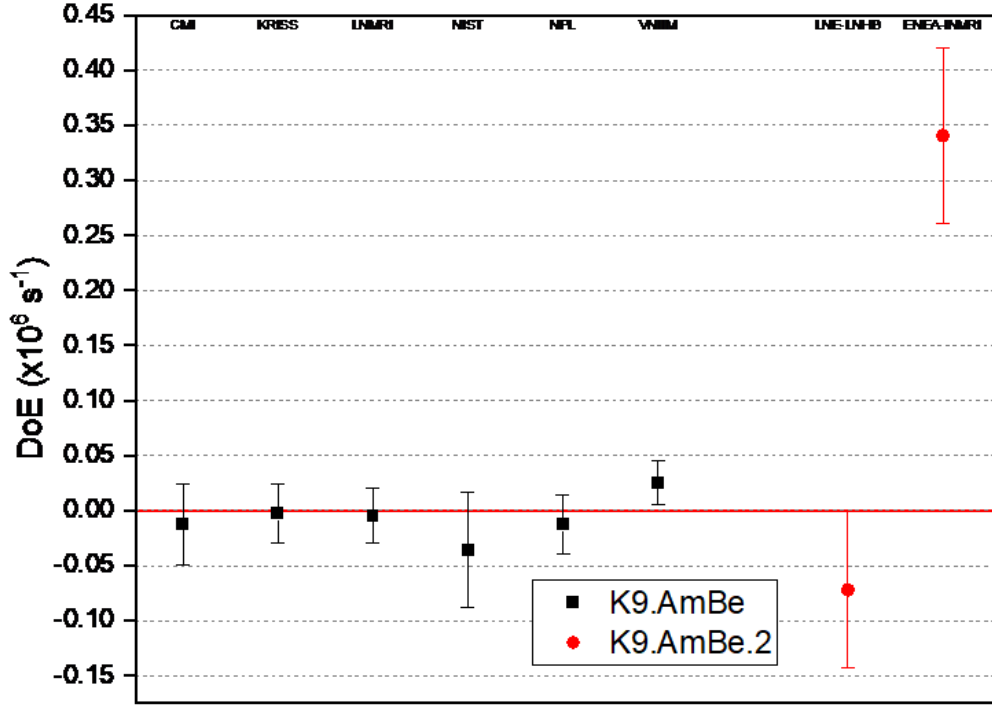


Figure 4: Degrees of Equivalence for the original K9.AmBe comparison and those linked to it through the subsequent K9.AmBe.2 comparison, with expanded ($k = 2$) uncertainties. All participants in the K9.AmBe comparison used the Mn bath technique, although the VNIIM value is a mean of the Mn bath and associated particle techniques. The correction factors for all K9.AmBe participants were based on ENDF/B-VI cross-sections, except for NIST and LNMRI whose were based on ENDF/B-V.

6 SUMMARY AND CONCLUSION

The subsequent comparison of neutron emission rate measurements, CCRI(III)-K9.AmBe.2, has concluded with ENEA-INMRI (Italy), LNHB (France) and NPL (UK) able to participate. All participants used the manganese bath technique to measure the neutron emission into 4π sr of an Am-Be source. The reported value of LNHB is consistent with that of NPL within the uncertainties, with the normalised error on the degree of equivalence equal to 0.934. However, the value from ENEA-INMRI was not consistent with that of NPL within the uncertainties, with the normalised errors on the degree of equivalence equal to 5.154. ENEA are therefore an outlier in this exercise.

ENEA-INMRI, after the completion of the report, checked its results by measuring in the MnSO_4 bath a certified NPL Am-Be source owned by itself. This allowed the performance of some useful tests on the measurement chain, to benchmark the Fluka Monte Carlo code used for the computation of all corrective factors, and finally to understand the origin of the deviation of its result in this comparison.

When linked to the KCRV of the original CCRI(III)-K9.AmBe comparison exercise, the unilateral degree of equivalence and expanded uncertainty for LNHB is $(-0.0719 \pm 0.0708) \times 10^6 \text{ s}^{-1}$.

7 ACKNOWLEDGEMENTS

The authors would like to thank Dr Steven Judge for collating and checking the participants' reports before the evaluation.

The evaluation of the intercomparison was funded by the UK National Measurement System Policy Unit.

8 APPENDICES

8.1 Uncertainty Budgets

Table 6: Full uncertainty budget for the ENEA-INMRI measurements

Source	Distribution	Uncertainty component (%)	Degrees of freedom
Counting	Normal	0.256	12
Counter efficiency, ϵ_{NaI}	Normal	0.955	1
Probability of neutron absorption by ^{55}Mn , ϵ_{Mn}	Normal	0.413	1E+07
Half-life of source	Normal	0.140	1
Combined standard uncertainty		1.07	
Expanded uncertainty		2.14	

Table 7: Full uncertainty budget for the LNE-LNHB measurement

Source	Comment	Uncertainty (%)	Type of uncertainties
γ -ray counting	Standard deviation of the mean of repeated measurements	0.9	A
γ -ray counter efficiency	Calibration	0.64	B
Neutron emission spectrum	Conservative estimation obtained by the difference between two spectra for AmBe	0.1	B
Neutron capture probability by the manganese	Conservative estimation obtained by the difference between MCNP6 and Tripoli-4	0.25	B
Combined uncertainty		1.1	
Expanded uncertainty		2.2	

Table 8: Full uncertainty budget for the NPL measurement

Source	Uncertainty (%)	Distribution	Sensitivity	Uncertainty component (%)	Degrees of freedom
Counting	0.05	Normal	1	0.05	∞
Cross-section ratio	0.2	Normal	1	0.20	∞
Efficiency	0.4	Normal	1	0.40	∞
O & S losses	20	Rectangular	0.03530	0.41	∞
Cavity and source capture	10	Rectangular	0.01471	0.08	∞
Leakage	4	Rectangular	0.01441	0.03	∞
Timing	0.05	Rectangular	1	0.03	∞
Mixing	0.2	Rectangular	1	0.12	∞
Solution concentration	0.1	Normal	1	0.10	9
Background	10	Normal	0.02713	0.27	9
Dead-time	10	Normal	0.0005	0.005	30
Half-life of source	0.15	Rectangular	0.0019	0.0002	∞
Combined standard uncertainty				0.69	368
Expanded uncertainty				1.38	

8.2 Anisotropy measurements

LNHB and NPL measured the anisotropy of the source in addition to the emission rate as part of the comparison exercise. LNHB made measurements at 15° steps from 0° to 180° , whereas NPL measured the anisotropy of the source in 10° steps from 0° to 180° . The convention used to define the angles around the source capsule is shown in Figure 5.

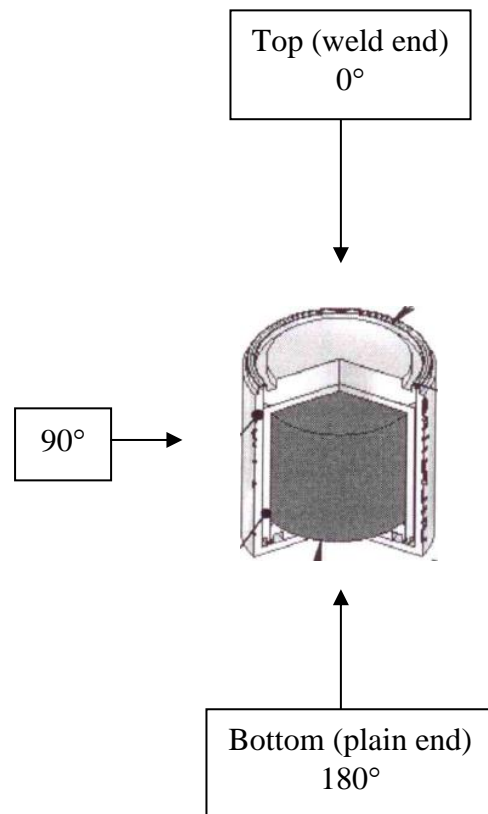


Figure 5: Anisotropy angle convention for the intercomparison source

8.2.1 LNHB

The anisotropy of the neutron source was measured using a BF_3 long counter at a distance from the source of about 1.5 m. The source was placed on a lightweight holder positioned on top of a rotating support with its cylindrical axis in the horizontal plane. A scatter correction was made by making measurements with a shadow cone positioned between the source and the long counter.

8.2.2 NPL

Measurements were made with both long counters available at NPL:

- A De Pangher long counter designed by De Pangher and Nichols⁹ with a 38 mm outer diameter BF_3 tube. The one in use at NPL is one of a batch of six made by Centronic in the late 1960s¹⁰.
- A McTaggart type¹¹, built at NPL, with a 50 mm outer diameter BF_3 tube for greater efficiency. From hereon it will be referred to as the NPL long counter.

Both long counters were nominally at 2 m from the source and scatter contributions were measured using a shadow cone and subtracted.

8.2.3 Results

The measurements of LNHB and NPL are shown in Figure 6. All are normalised to the sum of the angular measurements weighted according to the solid angle over the angular interval.

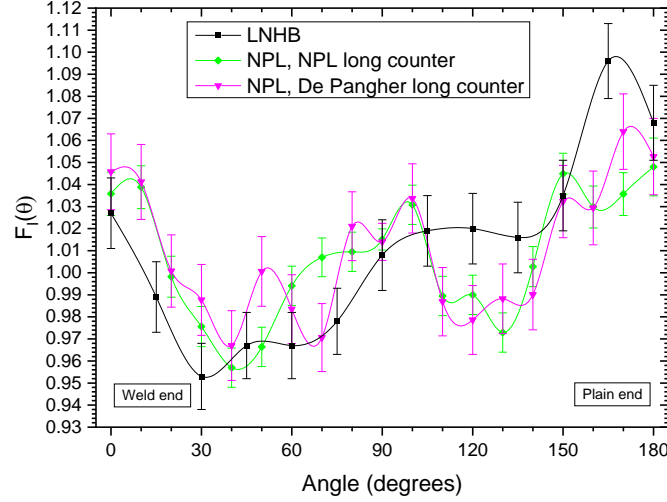


Figure 6: Graph of anisotropy factor vs angle
(error bars represent the total uncertainty at $k = 1$)

It can be seen that there is reasonably good agreement between LNHB and NPL over much of the angular range. The angle of most significance is 90° as this is the conventional angle for positioning any instrument or device being irradiated by the source. The anisotropy factors of each laboratory at 90° , $F(90^\circ)$, are given in Table 9 and plotted in Figure 7.

Table 9: Anisotropy factors at 90° with statistical uncertainties at $k = 1$

	$F(90^\circ)$
LNHB	1.008 ± 0.016
NPL (NPL LC)	1.0151 ± 0.0048
NPL (De Pangher LC)	1.0140 ± 0.0084

The weighted mean of the measured values is 1.0144 as shown in Figure 7. The error bars at $k = 1$ for all measurements straddle the weighted mean which represents excellent agreement.

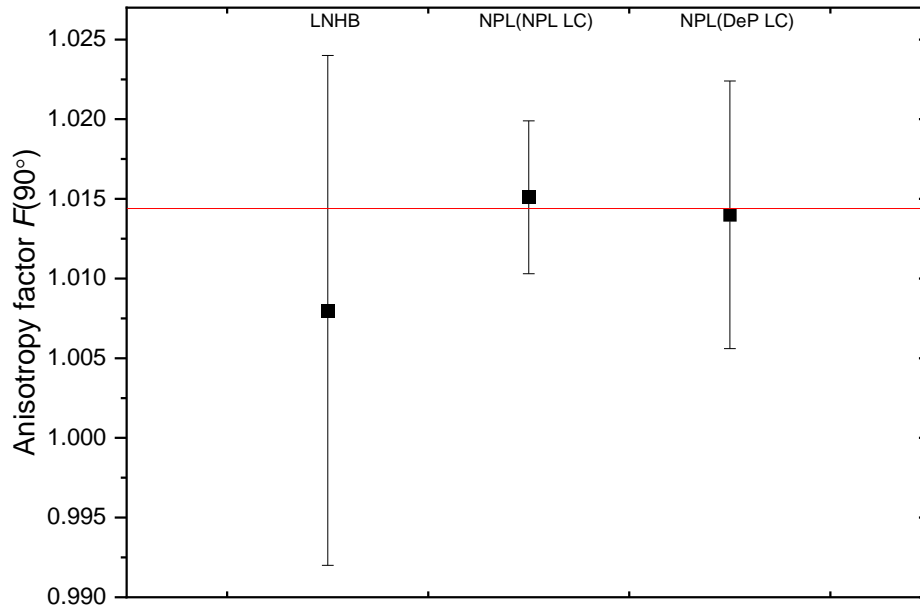


Figure 7: Comparison of anisotropy factors at 90 degrees. The red line represents the weighted mean of all 3 measurements
(error bars represent the statistical uncertainty at $k = 1$)

9 REFERENCES

- 1 N.J. Roberts, L.N. Jones, Z. Wang, Y. Liu, Q. Wang, X. Chen, H. Luo, C. Rong, M. Králik, H. Park, K.O. Choi, W.W. Pereira, E.S. da Fonseca, P. Cassette, M.S. Dewey, N.N. Moiseev and I.A. Kharitonov [NPL,CIAE,CMI,KRISS,LNMRI,LNE-LNHB,NIST,VNIIM] *International key comparison of measurements of neutron source emission rate (1999–2005): CCRI(III)-K9.AmBe*, Metrologia 48, Tech. Suppl., 06018 (2011), doi:[10.1088/0026-1394/48/1A/06018](https://doi.org/10.1088/0026-1394/48/1A/06018)
- 2 A. Ferrari, P.R. Sala, A. Fasso and J. Ranft 2005. *FLUKA: a multi-particle transport code*. CERN-2005-10 (2005), INFN/TC_05/11, SLAC-R-773. Version 2011.2x.6
- 3 P. Cassette, F. Ogheard and C. Thiam 2014. *Calibration of neutron sources emission rate with the manganese bath, using a new method for the on-line activity measurement of ^{56}Mn by Cerenkov-gamma coincidences*. Revue Française de métrologie. Volume 2014-4 N° 36 p. 39-54.
- 4 F. Ogheard, J.L. Chartier, P. Cassette 2012. *Monte Carlo simulation of the new LNHB manganese bath facility*. Applied Radiation and Isotopes, 70, 794-801.

-
- 5 MCNP: Monte Carlo N-Particle Transport Code System for Multi-particle and High Energy Applications, RSICC Computer Code, Collection Report CCC-715, LANL, Los Alamos.
 - 6 M Laliberté and W E Cooper, *Model for Calculating the Density of Aqueous Electrolyte Solutions*, J. Chem. Eng. Data 2004, 49, 1141-1151
 - 7 N.J. Roberts, L.N. Jones, *Recent developments in radionuclide neutron source emission rate measurements at the National Physical Laboratory*, Applied Radiation & Isotopes **68** (2010) 626-630, doi:[10.1016/j.apradiso.2009.09.023](https://doi.org/10.1016/j.apradiso.2009.09.023)
 - 8 N.J. Roberts, N.N. Moiseev and M. Králik, *Radionuclide neutron source characterization techniques*, Metrologia 48 No. 6, S239 –S253, 2011, doi:[10.1088/0026-1394/48/6/S02](https://doi.org/10.1088/0026-1394/48/6/S02).
 - 9 De Pangher J, and Nichols L L, *A Precision Long Counter for Measuring Fast Neutron Flux Density*, Pacific Northwest Laboratory Report BNWL-260, 1966.
 - 10 Marshall T O, *Some Tests on the Consistency of the Performance of Six Precision Long Counters Intended as Secondary Standards for the Measurement of Fast Neutron Flux Densities*, Health Physics **18**, 427-429, 1970.
 - 11 McTaggart M H, *A Study of the Neutron Long Counter*, AWRE report NR/A-1/59, 1959.